A Semi-automatic System for Measuring Tibial Cartilage Volume

James Cheong and David Suter
Dept. of Electrical and Computer Systems Engineering
Monash University
Clayton, Vic. 3800, Australia
{james.cheong ; d.suter}@eng.monash.edu.au

Flavia Cicuttini
Dept. of Epidemiology and Preventive Medicine
Monash University Medical School
Alfred Hospital, Prahan, Vic. 3181, Australia
flavia.cicuttini@med.monash.edu.au

Abstract—**Osteoarthritis is a chronic and crippling disease affecting an increasing number of people each year. With no known cure, it is expected to reach epidemic proportions in the coming years. Currently, there is strong interest in developing a fully automated cartilage area/volume measurement method in the medical field to assist both pharmaceutical companies and medical professions in researching the disease. This paper describes the development of a semi-automatic system for segmenting and measuring human knee cartilage volume from Magnetic resonance imaging (MRI) scans. The cartilage volume obtained from the semi-automated method has been benchmarked against the current gold standard (cartilage volume from manual segmentation).**

I. INTRODUCTION

According to the Arthritis Foundation of Australia, over 3.4 million Australians suffer from some form of arthritis. It is estimated that 16.7% of the population have some form of arthritis at a total cost of $11.2 billion to the community each year. Arthritis means "joint inflammation" and is a serious chronic condition with no known cure. There is currently an urgent need to better understand the disease, as arthritis is a major cause of disability and pain in Australia.

Osteoarthritis (OA) is the most common form of arthritis and involves the gradual break down and loss of articular (joint) cartilage. It affects about 14% of the adult population [1] and is most prevalent in the knee and hip joints. Recent studies have shown that knee cartilage volume can be measured accurately and reproducibly from MRI scans [2-4]. Radiologic assessment of joint space narrowing (JSN) is currently recommended as the best measure of OA progression and studies have shown that cartilage volume measured from MRI scans correlate with the radiographic grading of OA [5-7]. Changes in cartilage volume are currently being used as a marker to predict OA onset or progression, and such measurements are emerging as a possible measure of OA severity in the knee [8].

Quantifying cartilage volume in OA will enable evaluation of therapies that may slow down or stop cartilage degradation and also preventive OA developing. There is a strong demand to automate the measurement process because large-scale clinical trials and epidemiological studies will be needed to address these issues. Research by the team of the 3rd author (Cicuttini) at the Department of Epidemiology and Preventive Medicine indicate that measurement of the tibial cartilage alone is a valid indicator of cartilage volume [9, 10]. The tibial cartilage is a clearly defined anatomical structure and thus enables measurements that are easily reproducible. Measuring and segmenting the femoral cartilage is less reproducible and more inaccurate because it is a continuous structure and forms part of three joints, the patellofemoral, lateral tibiofemoral and medial tibiofemoral joints. The femoral cartilage articulates with the patella, medial and lateral tibial cartilages and this makes it difficult to find the most appropriate component to measure.

Current methods of cartilage volume measurement involve some form of manual segmentation carried out by a trained clinician. The key steps in this segmentation process involve delineating the cartilage and separating it from the surrounding tissues. Today, it is widely accepted that T1-weighted gradient echo sequences with spectral fat suppression displays cartilage with high contrast to surrounding tissue [11]. These sequences produce images in which the cartilage appear bright compared to all other tissue. Images of a patient's knee are obtained using MRI with such a setup. The scans obtained are greyscale images in the sagittal plane and consists typically of 60 images (slices) for each knee. Using some form of medical display software, the clinician will visually inspect and identify the presence of cartilage on each image slice. If cartilage is present, the cartilage boundary is manually traced, see Fig. 1. After all 60 slices have been processed, the cartilage volume can be estimated using Cavalieri's principle [12, 13], where the sum of the segmented cartilage area is multiplied by the inter-slice distance (slice thickness).

This manual process is laborious and can take up to 1 hour to process a single patient knee. It is also subject to the judgement of the clinician and requires significant experience and training to obtain accurate and reproducible results. These factors increase the demand for automating the segmentation process. There are currently a number of semi-automated segmentation methods that have been developed [14-19]. These usually involve a human operator initialising the procedure by setting a number of starting points for each slice where cartilage is present, followed by an automated segmentation process. Edge detection, active contours (snakes), template matching, and statistical models are some of the segmentation techniques used. We present in this paper a semi-automated

system that uses a segmentation method, based on directional Canny filters, to measure tibial cartilage volume.
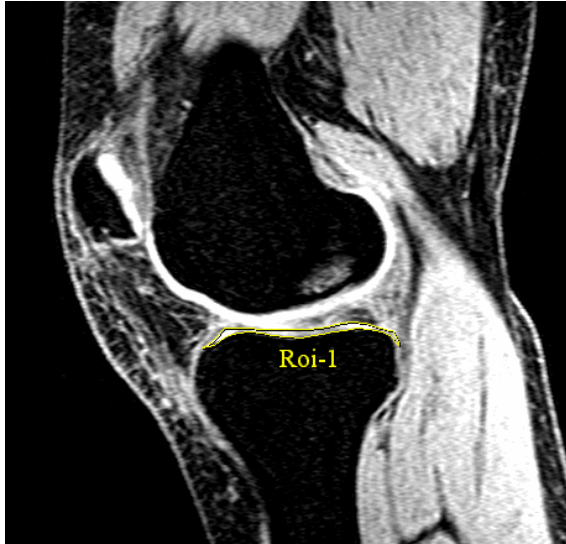

Figure 1.   A MRI of the knee in the sagittal plane, displaying tibial cartilage that has been manually segmented by a clinician.

The paper is organised as follows. In Section II, we provide an overview of the developed system and the implementation details of the segmentation method. In Section III, we present some results of the segmentation algorithm. Discussion and concluding remarks are given in Section IV and Section V respectively.

II.   MATERIALS AND METHODS

A.   Overview

We developed a semi-automatic system that is targeted at segmenting the tibial cartilage. Each image slice is segmented individually using an edge detection algorithm based on the Canny edge detector [20]. This segmentation method improves on the method proposed by Lynch [16] and was written in Java as a plugin for ImageJ [21]. The system has an interface that is compatible with DICOMDIR, allowing the user to work on a patient's MRI images directly without having to reassemble the corresponding patient slices in the correct order. The DICOM interface is available as a plugin developed under the GNU General Public License by Thomas Hacklaender [22].

The system requires users to have knowledge on human knee joints. If tibial cartilage is detected in an image, the user places 8 points close to one of the boundaries of the cartilage by clicking on the appropriate locations on the image. These points form a cubic spline, where the first and the last point are called "end points" and the points in between, "control points". The end points have to be placed with a bit of precision at each end of the tibial cartilage extremity while the control points can be placed loosely around the area of the cartilage boundary. This is because only the positions of the control points are optimised to detect the cartilage boundaries. When these points are placed in satisfactory positions, the segmentation algorithm is performed and the user is presented with an outline of the

tibial cartilage with an adjustable boundary. If this outline is not "correct", the user has the option of manually adjusting it. When the user is satisfied with the outline, the area of the segmented cartilage can be calculated and stored in a log file. The volume of the medial and lateral tibial cartilage can be calculated when all slices have been processed. This is done by multiplying the sum of the area data in the log file by the slice thickness.

B.   Implementation

The segmentation process involves 2 key steps that are transparent to the user. The basic idea of the first step is to locate a cubic spline that runs approximately along the center of the cartilage. This can be achieve by smoothing the image and locating pixels that return a high intensity value. The intuition is that cartilage regions generally have higher intensity values compared to the surrounding bone/tissue, which have much lower intensity values. Therefore, by smoothing the image, the boundaries of the cartilage will be blurred and decrease in intensity due to the surrounding bone/tissue while the middle region of the cartilage will still contain pixels of high intensity. By locating these pixels of high intensity in the blurred image, we can locate the middle of the cartilage.

When the middle of the cartilage is detected, the next step is to detect the boundaries of the cartilage. For the tibial cartilage, two boundaries have to be detected, the bone-cartilage interface (lower boundary) and the boundary closest to the femur (upper boundary). The basic idea in this second step is to drive two cubic splines in opposite directions from the middle of the cartilage, each towards one of the cartilage boundaries. This is achieve by exploiting the characteristic shape of the tibial cartilage and the intensity values of the surrounding bone/tissue structure. In a large proportion of the MRI scans, the tibial cartilage appears as a horizontal strip of cartilage of high pixel intensity, surrounded by bone/tissue of lower pixel intensity. By calculating the image gradient in the y-axis, the two boundaries of the tibial cartilage can be differentiated and located due to the opposing values of the image gradient at each boundary.

To implement the first step, the original image is smoothed from a coarse to fine scale using a Gaussian filter and optimising a cost function calculated from the filter responses, refer to (1). The purpose of this cost function is to detect the optimal positions for the control points of the center spline. Firstly, 5 evenly distributed points are inserted between each of the 8 points placed by the user, and the Gaussian filter response at each of these 43 points is summed. Because the length of the tibial cartilage is not large, placing more than 5 points between each point might result in repeated points. The cost function is then iteratively minimised by altering the position of the control points and recalculating the effect on the cost function. The positions of the end points are fixed, thus only the positions of the control points are moved. The 4 possible positions for the control point being adjusted are inward and outward perpendicular to the local spline direction, and in the two directions parallel to the local tangent to the spline. When the cost function cannot be reduced any further, the process stops. This optimisation process is run twice, the first time

using a coarse scale Gaussian filter ($\sigma = 2$) and adjusting the control points by 2 pixels; and the second time using a finer scale Gaussian filter ($\sigma = 1$) and adjusting the control points by 1 pixel.

$$cost = \frac{-\sum \text{Filter Response}}{A \times (\text{Resultant Spline Length})} \quad (1)$$

To implement the second step, an optimisation algorithm similar to that previously described is used. Instead of Gaussian filters, directionally oriented Canny filters are used. The "normal" Canny edge detector [20] finds edges by looking for local maxima of the image gradient. The image gradient ∇R is calculated using the derivative of a Gaussian filter and is defined as:

$$\nabla R = [R_x, R_y], \quad (2)$$

where R_x = filter response in the x direction and R_y = filter response in the y direction. In the case of directional Canny edge detection, the filter response $R(\Theta)$ is defined as:

$$R(\Theta) = R_x \cos\Theta + R_y \sin\Theta \quad (3)$$

Edges at the specified angle Θ return a positive filter response, while edges at ($\Theta+180^o$) return a negative filter response. See Fig. 2, where grey areas represent a value close to zero, white areas represent strong positive values and black areas, strong negative values. NOTE: $\Theta = 0^o$ is horizontal with increasing x and $\Theta = 90^o$ is vertical with increasing y. We set $\Theta=90^o$, thus eliminating the response in the horizontal x axis and including only the vertical response of the y axis. This enables the detection of the lower and upper boundaries of the cartilage from the sign of the filter response because when $\Theta=90^o$, the response of the directional Canny filter returns values that are opposite in sign on either side of the tibial cartilage boundary, see Fig. 2.

The cost function for the second optimisation algorithm is the same as that used to detect the center spline. 5 evenly distributed points are inserted once again between the 8 points that define each spline. The directional Canny filter response with Θ set to 90° is calculated and the response for each of the 43 points are summed and divided by the length of the resulting spline. To detect the lower boundary, the filter response is multiplied by –1, while for the upper boundary, the filter response is left as it is. Similarly, the cost function is iteratively optimised for the lower and upper boundaries by altering the position of the control points. When the cost function cannot be reduced any further or when an upper limit for the number of iterations is reached, the process stops. The upper limit minimises the deviation of the spline from the actual cartilage boundary and must be large enough so that it does not stop the optimisation prematurely. The optimisation algorithm is run twice, the first time using a coarse scale ($\sigma = 2$) to calculate the image gradient and the second time using a

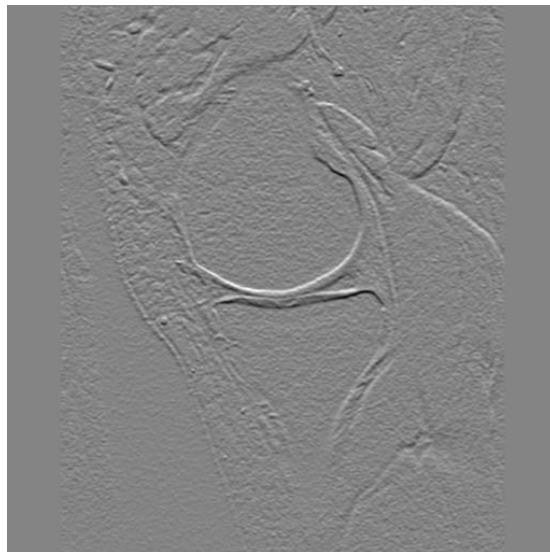finer scale ($\sigma = 1$). The control points are adjusted by 1 pixel for both cases.

Figure 2.   Directional Canny filter response, with $\Theta=90^o$

The segmented cartilage area is calculated by multiplying the pixel height and width by the number of pixels within the boundary outline. The volume of the medial and lateral tibial cartilage for a patient is then calculated by summing the corresponding cartilage areas and multiplying by the slice thickness. The dimensions of the pixel height, pixel width, and slice thickness are obtained from the metadata in the MRI images.

III.   RESULTS

Experiments were performed to determine the segmentation and measurement accuracy of our method. Both segmentation accuracy and measurement accuracy were determined by comparing the cartilage area collected from our method with those derived by the manual method. The difference between segmentation and measurement accuracy is that for segmentation accuracy, the user does not manually adjust the detected boundaries if they do not "correctly" outline the cartilage. With measurement accuracy, the user has the option of adjusting the boundaries before recording the area measurements. Fig. 3 and Fig. 4 show the steps involve segmenting this cartilage using our semi-automatic method.
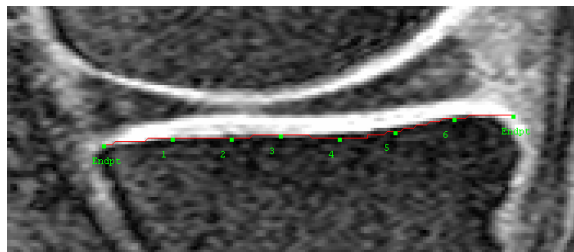

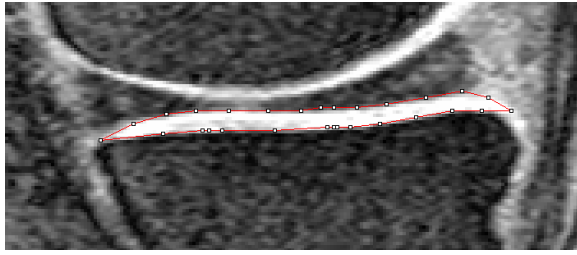Figure 3.   User places 2 end points and 6 control points.

Figure 4. Tibial cartilage segmented without user adjustments

Fig. 5 compares the cartilage area measured using the manual method and our semi-automatic method from a patient knee. This figure shows that the manual and semi-automatic measurement methods measure the same pattern of cartilage area within the joint.

To examine the relationship between the measurements, a regression between the paired measurements from our method and the manual method was performed, see Fig. 6 and Fig. 7. The linear regression line in Fig. 6 shows strong correlation between the measurements of the manual and our semi-automatic segmentation method when the user can manually correct the boundaries. If the boundaries were not adjusted, the linear regression line still shows a good correlation between the measurements, see Fig. 7. However, this correlation is not as strong as when the boundaries are manually adjusted.

The results obtained correspond well with those measured using the manual method. In addition, we found that our semi-automatic method of segmentation can reduce the time taken to process a single patient knee. Initial testing indicated around 30 min to process a patient, compared to 60 min using the manual method. These figures are rough estimates and more precise data have to be collected to validate them. The users were also in the process of learning the operation of the system when these timings were taken. With more familiarity, the time taken should be even shorter.
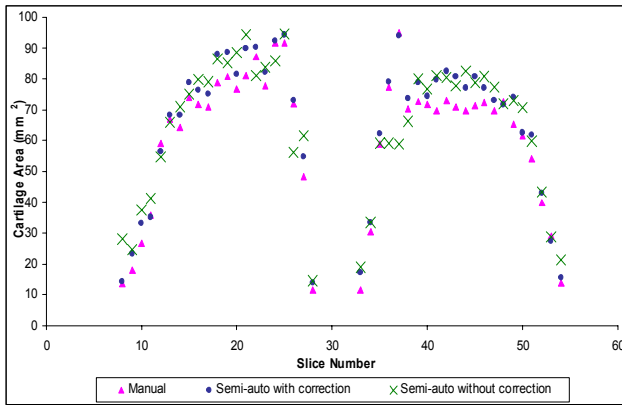

Figure 5. Comparison of manual and semi-automated measurements for a patient. Image sequence is from medial (lower slice numbers) to lateral (higher slice numbers) for this patient knee.
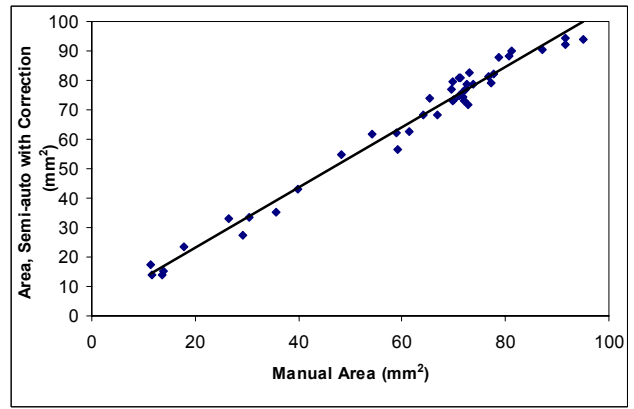

Figure 6. Relationship between areas measured from manual and semi-automated method. The linear regression line yielded R2=0.98, slope=1.02, y-intercept=2.70.
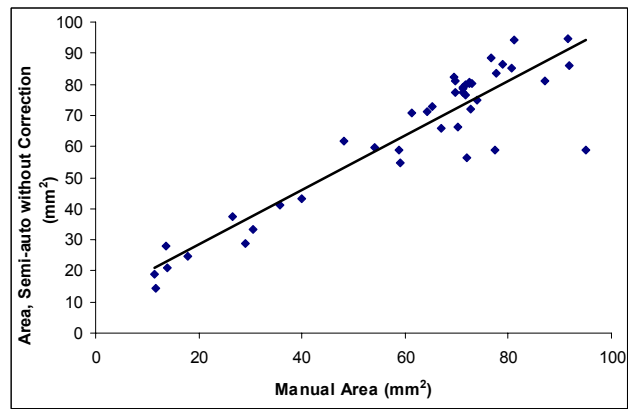

Figure 7. Relationship between areas segmented from manual and semi-automated method. Boundaries from semi-automated method have not been adjusted by user. The linear regression line yielded R^2=0.84, slope=0.87 and y-intercept=11.23.

IV. DISCUSSION

Our data have shown that the semi-automatic method displays a high degree of measurement and segmentation accuracy. The other segmentation techniques mentioned in Section I focus on segmenting the femoral cartilage and only present results from a small number of patients, or in some cases, only a few MRI slices. This makes it difficult to compare their results with our own.

Our segmentation method is an improved and simplified implementation of Lynch's segmentation technique that is targeted at segmenting tibial cartilage. Our method produces better results than Lynch's method when applied on tibial cartilage. Lynch's segmentation technique, as described in [16], is not very clear on the implementation details. According to his description, the cost function to detect the cartilage boundary is calculated by obtaining the sum of directional Canny filter responses of points inserted between user placed control points, and dividing these responses by the length of the spline between the control points. The angle Θ, for each of the

directional Canny filter response is oriented to be parallel to the angle between the local spline direction for each relevant point and the x-axis, θ. To detect the bone-cartilage (lower) boundary, the directional canny filter response is multiplied by -1 when $0^o <= \theta < 90^o$ or $180^o <= \theta < 270^o$. To detect the upper boundary, the directional canny filter response is multiplied by -1 when $90^o <= \theta < 180^o$ or $270^o <= \theta < 360^o$. This description of Lynch's method was implemented and we obtained results that did not correspond with what was expected. Some of the control points of the lower boundary are incorrectly located on the upper boundary and vice versa for the control points of the upper boundary. This causes the boundaries to cut across each other's path and produce an erroneous segmentation, see Fig. 8 and Fig. 9.

A common problem encountered during segmentation of cartilage is the non uniform texture of cartilage. This is due to the biochemically heterogeneous property of cartilage. From our library of MRI images, the range of 8 bit greyscale pixel intensities that define the tibial cartilage region can be from 70 to 255 for a single slice, see Fig. 10. This causes inconsistent image gradients even after smoothing, and this can lead to one of the control points latching onto an incorrect position and iterating away from the boundary, resulting in an incorrect segmentation.

Another common problem encountered with segmenting cartilage occurs when processing images where the femoral and tibial cartilages are in contact, see Fig. 11. Because some parts of the cartilage are actually in contact, there is no edge information for the upper boundary of the tibial cartilage. This causes the algorithm to steer towards the bone-cartilage boundary of the femoral cartilage instead.

In most cases, the segmentation method works well and little or no adjustments are required to correct the outline. The number of slices where incorrect segmentation occurs for a patient knee is highly dependent on the set up of the MRI scanner. In MRI, the tissue contrast can be adjusted by selecting different types of pulse sequences and by changing the parameters of these sequences such as repetition time, echo time, flip angle, etc. Even though it is widely accepted that T1-weighted gradient echo sequences with spectral fat suppression visualises cartilage with high contrast to surrounding tissue, there is no agreed setting for repetition time, echo time and flip angle. This leads to MRI images with varying tissue contrast between patients and this is a common problem encountered by data driven segmentation methods such as ours.

A final comment about our method is the inflexibility of having a fixed number of control points. In most cases, 6 controls points can clearly represent the shape of the tibial cartilage due to a lack of curvature. However, in some slices, the area of the cartilage can be very small and fitting 6 control points to these images are a bit more difficult. A solution to this problem would be to introduce some function that enables the user to define the maximum number of control points. This would involve more user interaction, but would increase the accuracy of the method.
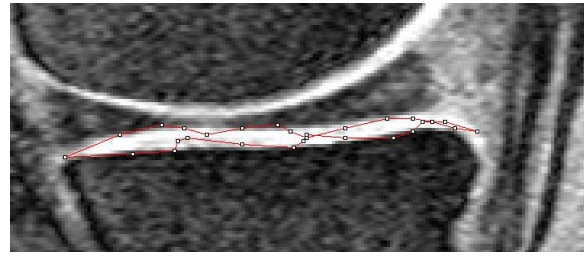

Figure 8.   Tibial cartilage boundaries detected by Lynch's implementation.
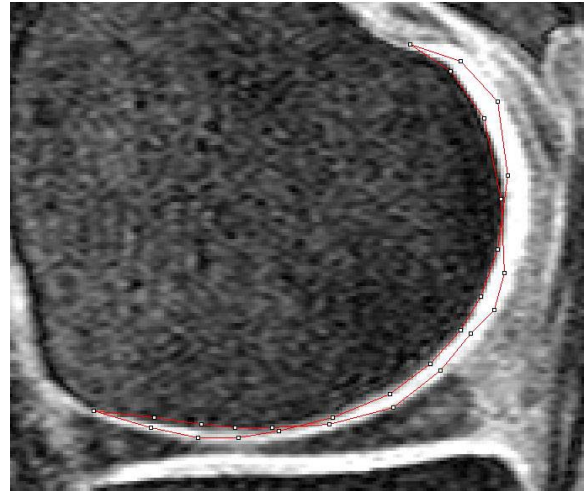

Figure 9.   Femoral cartilage boundaries detected by Lynch's implementation.
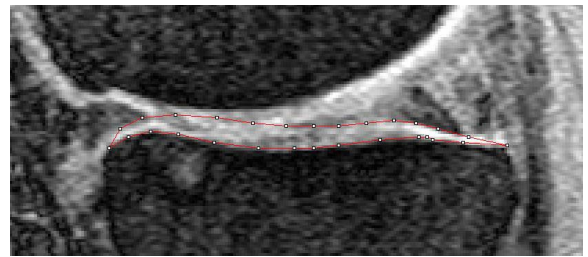

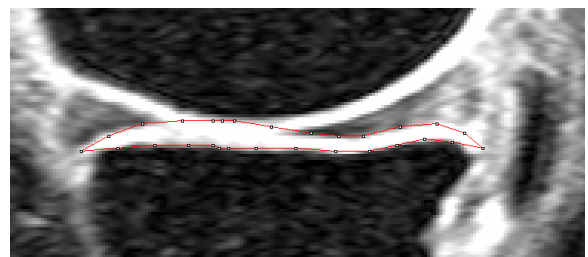Figure 10.   Example of incorrect segmentation due to non uniform texture.

Figure 11.   Example of incorrect segmentation due to cartilage touching.

V.   CONCLUSION AND FURTHER WORK

We have developed a semi-automatic system for quantitating knee cartilage volume. The segmentation method has been tested and compared with the current "gold" standard

of manual measurements and has displayed a high degree of measurement and segmentation accuracy.

There are a number of cases when using data driven segmentation methods such as our semi-automatic method leads to incorrect segmentation. We intend to overcome these problems and develop a more accurate segmentation method by using model based segmentation methods such as Active Shape Models (ASM). To date we have only examined our segmentation method on healthy knees. We intend to test the segmentation method on MRI images of osteoarthritic knee, where cartilage edges may be less well defined.

REFERENCES

[1] M. D. Forman, R. Malamet, and D. Kaplan, "A survey of osteoarthritis of the knee in the elderly," *The Journal of Rheumatology*, vol. 10, pp. 282-287, 1983.

[2] F. Eckstein, J. Westhoff, H. Sittek, K.-P. Maag, M. Haubner, S. Faber, Englemeier K-H., and M. Reiser, "In vivo reproducibility of three-dimensional cartilage volume and thickness measurements with MR imaging," *American Journal of Roentgenology*, vol. 170, pp. 593-597, 1998.

[3] F. Cicuttini, A. Forbes, K. Morris, S. Darling, M. Bailey, and S. Stuckey, "Gender differences in knee cartilage volume as measured by magnetic resonance imaging," *Osteoarthritis and Cartilage*, vol. 7, pp. 265-271, 1999.

[4] G. Jones, M. Glisson, K. Hynes, and F. Cicuttini, "Sex and site differences in cartilage development: a possible explanation for variations in knee osteoarthritis in later life," *Arthritis & Rheumatism*, vol. 43, pp. 2543-2549, 2000.

[5] M. Glisson, A. Forbes, K. Morris, S. Stuckey, and F. Cicuttini, "Comparison of x-rays and magnetic resonance imaging in the definition of tibiofemoral joint osteoarthritis," *Radiography*, vol. 6, pp. 205-209, 2000.

[6] F. Eckstein, F. Cicuttini, J. P. Raynauld, J. C. Waterton, and C. Peterfy, "MRI of articular cartilage in knee osteoarthritis: morphological assessment," unpublished.

[7] F. Cicuttini, A. E. Wluka, A. Forbes, and R. Wolfe, "Comparison of tibial cartilage volume and radiologic grade of the tibiofemoral joint," *Arthritis & Rheumatism*, vol. 48, pp. 682-688, 2003.

[8] J. P. Raynauld, "Magnetic resonance imaging of articular cartilage: toward a redefinition of "primary" knee osteoarthritis and its progression," *The Journal of Rheumatology*, vol. 29, pp. 1809-1810, 2002.

[9] F. Cicuttini, A. E. Wluka, and S. L. Stuckey, "Tibial and femoral cartilage changes in knee osteoarthritis," *Annals of the Rheumatic Diseases*, vol. 60, pp. 977-980, 2001.

[10] F. Cicuttini, A. E. Wluka, Y. Wang, and S. L. Stuckey, "Longitudinal study of changes in tibial and femoral cartilage in knee osteoarthritis," *Arthritis & Rheumatism*, vol. 50, pp. 5-9, 2004.

[11] M. P. Recht, J. Kramer, S. Marcelis, M. N. Pathria, D. Trudell, P. Haghighi, D. J. Sartoris, and D. Resnick, "Abnormalities of articular cartilage in the knee: analysis of available MR techniques," *Radiology*, vol. 187, pp. 473-478, 1993.

[12] B. Caverlieri, *Geometria Indivisibilibus Continuorum*: Bononi: Typis Clemetis Feronij, 1635. Reprinted as Geometria degli Indivisibili. Torino: Unione Tipografico-Editorice Torinese, 1966.

[13] N. Roberts, "Unbiased estimations of volume: some notes for ANALYZE ™ users," in *Biomedical Imaging Resource, ANALYZE Reference Manual. Revision 7.5*. Rochester, Minnesota: Mayo Foundation, 1996, pp. III 302-307.

[14] Z. A. Cohen, D. M. McCarthy, S. D. Kwak, P. Legrand, F. Fogarasi, E. J. Ciaccio, and G. A. Ateshian, "Knee cartilage topograhpy, thickness, and contact areas from MRI: in-vitro calibration and in-vivo measurements," *Osteoarthritis and Cartilage*, vol. 7, pp. 95-109, 1999.

[15] A. A. Kshirsagar, P. J. Watson, J. A. Tyler, and L. D. Hall, "Quantitation of articular cartilage dimensions by computer analysis of 3D MR images of human knee joints," *Proceedings of the 19th Annual International Conference of the IEEE Engineering in Medicine and Biology Society*, vol. 19, pp. 753-756, 1997.

[16] J. A. Lynch, S. Zaim, J. Zhao, A. Stork, C. G. Peterfy, and H. K. Genant, "Cartilage segmentation of 3D MRI scans of the osteoarthritic knee combining user knowledge and active contours," *Proceedings of SPIE*, vol. 3979, pp. 925-935, 2000.

[17] T. Stammberger, F. Eckstein, M. Michaelis, K.-H. Englmeier, and M. Reiser, "Interobserver reproducibility of quantitative cartilage measurements: comparison of B-spline snakes and manual segmentation," *Magnetic Resonance Imaging*, vol. 17, pp. 1033-1042, 1999.

[18] S. K. Warfield, M. Kaus, F. A. Jolesz, and R. Kikinis, "Adaptive, template moderated, spatially varying statistical classification," *Medical Image Analysis*, vol. 4, pp. 43-55, 2000.

[19] S. Solloway, C. J. Taylor, C. E. Hutchinson, and J. C. Waterton, "Quantification of articular cartilage from MR images using active shape models," *Proceedings of the 4th European Conference on Computer Vision*, vol. 2, pp. 400-411, 1996.

[20] J. Canny, "A computational approach to edge detection," *IEEE Transactions on Pattern Analysis and Machine Intelligence*, vol. 8, pp. 679-698, 1986.

[21] W. S. Rasband, "ImageJ." National Institutes of Health, Bethesda, Maryland, USA: http://rsb.info.nih.gov/ij/, 1997-2005.

[22] T. Hacklaender, "DICOM import and export plugins." http://www.iftm.de/dicom/dcmimex.htm, 2004.